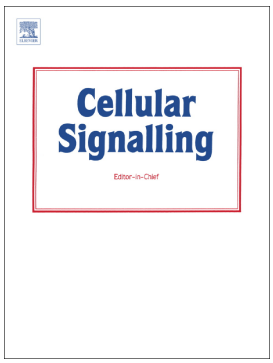

Diindolylmethane and its halogenated derivatives induce protective autophagy in human prostate cancer cells via induction of the oncogenic protein AEG-1 and activation of AMP-dependent kinase (AMPK)

Hossam Draz, Alexander A. Goldberg, Vladimir I. Titorenko, Emma Guns, Stephen H. Safe, J. Thomas Sanderson

PII: S0898-6568(17)30240-1
DOI: doi: 10.1016/j.cellsig.2017.09.006
Reference: CLS 8989

To appear in: *Cellular Signalling*

Received date: 8 May 2017
Revised date: 21 August 2017
Accepted date: 14 September 2017

Please cite this article as: Hossam Draz, Alexander A. Goldberg, Vladimir I. Titorenko, Emma Guns, Stephen H. Safe, J. Thomas Sanderson , Diindolylmethane and its halogenated derivatives induce protective autophagy in human prostate cancer cells via induction of the oncogenic protein AEG-1 and activation of AMP-dependent kinase (AMPK), *Cellular Signalling* (2017), doi: 10.1016/j.cellsig.2017.09.006

Diindolylmethane and its halogenated derivatives induce protective autophagy in human prostate cancer cells via induction of the oncogenic protein AEG-1 and activation of AMP-dependent kinase (AMPK)

Hossam Draz[1,2], Alexander A. Goldberg[1,3], Vladimir I. Titorenko[4], Emma Guns[5] Stephen H. Safe[6] and J. Thomas Sanderson[1,*]

[1] *INRS-Institut Armand-Frappier, Laval, QC, Canada.*

[2] *Department of Biochemistry, National Research Centre, Dokki, Cairo, Egypt.*

[3]*Critical Care Division and Meakins-Christie Laboratories, Faculty of Medicine, McGill University, Montréal, QC, Canada*

[4] *Department of Biology, Concordia University, Montréal, QC, Canada.*

[5] *The Prostate Centre, University of British Columbia, Vancouver, BC, Canada.*

[6] *Veterinary Physiology and Pharmacology, Texas A&M University, College Station, TX, United States.*

Key words: *Prostate cancer, LNCaP, C42B, autophagy, AMPK, AEG-1.*

Short title: Mechanism of DIM- and ring-DIM-mediated autophagy.

*Correspondence should be addressed to:

J. Thomas Sanderson

INRS-Institut Armand-Frappier

531 boulevard des Prairies

Laval, QC, H7V 1B7, Canada

Tel: +1 450-687-5010

Email: thomas.sanderson@iaf.inrs.ca

ABSTRACT

3,3'-Diindolylmethane (DIM) and its synthetic halogenated derivatives 4,4'-Br_2- and 7,7'-Cl_2DIM (ring-DIMs) have recently been shown to induce protective autophagy in human prostate cancer cells. The mechanisms by which DIM and ring-DIMs induce autophagy have not been elucidated. As DIM is a mitochondrial ATP-synthase inhibitor, we hypothesized that DIM and ring-DIMs induce autophagy via alteration of intracellular AMP/ATP ratios and activation of AMPK signaling in prostate cancer cells. We found that DIM and ring-DIMs induced autophagy was accompanied by increased autophagic vacuole formation and conversion of LC3BI to LC3BII in LNCaP and C42B human prostate cancer cells. DIM and ring-DIMs also induced AMP-activated protein kinase (AMPK), ULK-1 (unc-51-like autophagy activating kinase 1; Atg1) and acetyl-CoA carboxylase (ACC) phosphorylation in a time-dependent manner. DIM and the ring-DIMs time-dependently induced the oncogenic protein astrocyte-elevated gene 1 (AEG-1) in LNCaP and C42B cells. Downregulation of AEG-1 or AMPK inhibited DIM- and ring-DIM-induced autophagy. Pretreatment with ULK1 inhibitor MRT 67307 or siRNAs targeting either *AEG-1* or *AMPK* potentiated the cytotoxicity of DIM and ring-DIMs. Interestingly, downregulation of AEG-1 induced senescence in cells treated with overtly cytotoxic concentrations of DIM or ring-DIMs and inhibited the onset of apoptosis in response to these compounds. In summary, we have identified a novel mechanism for DIM- and ring-DIM-induced protective autophagy, via induction of AEG-1 and subsequent activation of AMPK. Our findings could facilitate the development of novel drug therapies for prostate cancer that include selective autophagy inhibitors as adjuvants.

1. INTRODUCTION

Prostate cancer is a major health problem worldwide, ranking as the second most common cancer in males [1] and the third leading cause of cancer-related deaths among American and Canadian men [2]. Treatment with drugs targeting androgen receptor signaling is the main therapy for early-stage androgen-dependent (AD) prostate cancer [3]. Unfortunately, many patients with AD prostate cancer will progress to an androgen-independent (AI) phenotype which is harder to treat and often fatal [4, 5]. Diindolylmethane (DIM) is a promising anticancer agent derived from the ingestion of *Brassica* plants (cabbage, broccoli, etc.) [6]. We have shown that several di-halogenated analogs of DIM (ring-DIMs) have anti-androgenic effects in human AD LNCaP prostate cancer cells [7] and induce apoptosis and necrosis in LNCaP and human AI PC-3 prostate cancer cells with greater potencies than DIM [8]. More recently, we have shown that DIM and ring-DIMs induce ER stress, mitochondrial dysfunction and autophagy in prostate cancer cells [9]. Autophagy is a self-digestion process activated by cellular stress, in which dysfunctional organelles and protein aggregates are sequestered in double-membraned vesicles[10], and then transported to lysosomes for proteolytic degradation and recycling to maintain cellular homeostasis [11].

Autophagy plays an important role in cancer cell progression; its induction in response to stresses following chemotherapy may promote cancer cell survival. However, excessive autophagy could activate a cell death mechanism known as cytotoxic autophagy, which is different from programmed cell death (apoptosis) [12, 13]. Uncontrolled growth of cancer cells is due to the inactivation of cell death pathways, such as apoptosis, and stimulation of cell survival pathways [14]. Thus, the dysregulation of autophagic machinery in cancer cells, leading to imbalances in the activation of cell death- or survival-related pathways, may have a critical influence on either

tumor progression or regression. Various Atg (autophagy-related) proteins are involved in initiation and regulation of autophagy [15].The conversion of LC3B (Atg3) from its diffuse LC3BI form into the punctuated LC3BII, which associates with the autophagosome [16], is used as a classic marker of autophagy. AMP-activated protein kinase (AMPK) regulates autophagy via phosphorylation of the autophagy-initiating protein ULK1 (Atg1) [17]. The oncogenic protein, astrocyte elevated gene-1 (AEG-1), also known as metadherin (MTDH) or protein LYRIC, is overexpressed in various cancer including that of the prostate [18, 19], where it acts as a mediator of AMPK activity and autophagy in response to cellular metabolic stress [20, 21]. AEG-1 contributes to chemoresistance in hepatocellular carcinoma (HCC) cells [22] and promotes hepato-carcinogenisis through inhibition of senescence in transgenic mice that overexpress hepatocyte-specific AEG-1 [23].

Although DIM is known to be a mitochondrial ATP synthase inhibitor [24] that alters AMP/ATP ratios leading to activation of AMPK [25], the exact mechanism(s) of DIM-induced protective autophagy has not been elucidated. Previous studies have shown that AEG-1 induces protective autophagy via activation of AMPK [21]. Therefore, we wished to determine the possible involvement of AEG-1 in AMPK activation as well as DIM- and ring-DIM-mediated induction of autophagy.

2. MATERIALS AND METHODS

2.1. Cell culture and treatment

LNCaP androgen receptor-(AR)-positive and AD human prostate cancer cells were purchased from the American Type Culture Collection (Manassas, VA); LNCaP C4-2B (C42B) AR-positive and AI human prostate cancer cells were purchased from the MD Anderson Cancer Centre (Houston, TX). LNCaP and C42B prostate cancer cells were cultured in RPMI 1640 medium

supplemented with 10% FBS, 1% penicillin/streptomycin (Life Technologies, Gaithersburg, MD) at 37°C and 5% CO_2. Ring-DIMs were synthesized in our laboratories as previously described [8].

For cell treatments, LNCaP and C42B were seeded in 24-well CellBind culture plates (Corning Inc., Corning, NY) at a density of 1.5 x 10^5 cells/well in RPMI 1640 supplemented with 2% dextran-coated charcoal-stripped FBS (Hyclone, Logan, UT); LNCaP cell medium was supplemented with 0.1 nM dihyrotestosterone (DHT; Steraloids Inc., Newport, RI). Cells were then treated with either DIM, ring-DIMs, or DMSO vehicle control (0.1% or 0.2% in the case of co-exposures). The ULK1 inhibitor MRT 67307 (Sigma-Aldrich, St-Louis, MO) was added to cell cultures four hours prior to treatment.

2.2. Cell death assay

For cell death measurements, LNCaP and C42B cells were treated with DIM, ring-DIMs, or vehicle control (DMSO). After 24 h of exposure, Hoechst 33342 (Sigma-Aldrich) and propidium iodide (PI; Invitrogen, Carlsbad, CA) stains were both added to each well at a concentration of 1 µg/ml for 15 min at 37^{o}C to detect apoptotic and necrotic (or late-apoptotic) cell death, respectively. Hoechst- and PI-positive cells were counted under a Nikon Eclipse (TE-2000U) inverted fluorescence microscope at 20x magnification using filter cubes with excitation wavelengths of 330-380 and 532-587 nm, respectively. Intact (viable) cells were counted as exhibiting neither Hoechst- (chromatin condensation/fragmentation) nor PI (cell membrane disintegration) staining. Subtoxic concentrations used for cell death analysis were as follows: 10 µM for DIM, 5 µM for both 4,4'-Br_2DIM and 7,7'-Cl_2DIM in LNCaP cells; then 20 µM for DIM, 10 µM for both 4,4'-Br_2DIM and 7,7'-Cl_2DIM in C42B cells. On the other hand, toxic concentrations used for cell death analysis were as follows: 20 µM for DIM, 15 µM for both 4,4'-

Br_2DIM and 7,7'-Cl_2DIM in LNCaP cells; then, 30 µM for DIM, 15 µM for 4,4'-Br_2DIM and 20 µM 7,7'-Cl_2DIM in C42B cells. At least 100 cells per treatment were examined.

2.3 Cell Proliferation assay

The effect of AEG-1 siRNA on cell proliferation of LNCap and C42B cells treated with DIM was determined using a WST-1 kit (Roche, Basel, Switzerland) which measures mitochondrial reductase activity of viable cells. LNCaP and primary C42B cells were plated in 96-well CellBind plates p (Corning Inc.) at a density of 1 x 10^3 cells/well in their appropriate culture medium for 24 h. Cells were then incubated with WST-1 substrate for 2 h and the formation of formezan was then measured using the absorbance at 440 nm with SpectraMax M5 spectrophotometer (Molecular Devices, Sunnyvale, California).

2.4. Autophagic vacuole detection

Autophagic vacuoles were measured using a Cyto-ID Autophagy detection kit (Enzo Life Sciences, Farmingdale, NY) according to the manufacturer's protocol. Cells were cultured in 24 well plates and treated with DIM or ring-DIMs for 24 h. Cells were washed with 1X assay buffer, then stained with CYTO-ID green detection reagent. Plates were protected from light and incubated for 30 minutes at 37°C.

Cells were counterstained with Hoechst 33342 and the number of autophagic vacuoles per cell were counted in vehicle control (DMSO), DIM- and ring-DIM-treated cells under a Nikon Eclipse inverted fluorescence microscope. At least 50 cells per treatment were counted.

2.5. Gene silencing with small interfering RNA (siRNA)

LNCaP and C42B cells underwent reverse transfection with SMARTpool siRNA oligonucleotides (a mixture of 4 siRNA; Dharmacon, Lafayette, CO) targeting either AMPK or *AEG-1* gene expression. Lipofectamine RNAiMAX reagent (Life Technologies) was used for the

reverse transfection of cells in serum free Opti-MEM medium (Life Technologies) according to the manufacturer's protocol.

2.6. Immunoblotting

Cells were treated with DIM, ring-DIMs or DMSO in 6-well CellBind culture plates (Corning Inc.) at a density of 7.5 x 10^5 cells/well. Cells were harvested using RIPA buffer (Pierce Biotechnologies, Rockford, IL) containing protease inhibitor cocktail and Halt phosphatase inhibitor (ThermoFisher, Waltham, MA). Protein concentrations were measured in cell lysates using a Pierce BCA protein assay kit (ThermoFisher). Twenty-five microgram aliquots of protein underwent electrophoresis on 10% sodium dodecyl sulfate-polyacrylamide gels and were then transferred to polyvinylidene difluoride (PVDF) membranes using a Trans-Blot Turbo Transfer System (Bio-Rad, Mississauga, ON). Rabbit primary antibodies for phospho-AMPK (T172), AMPK (23A3), phospho- acetyl-CoA carboxylase (pACC) (S79), ACC (C83B10), phospho-UlK1 (D1H4) and mouse primary antibodies for AEG-1 (2F11C3) and β-actin (8H10D10) were purchased from Cell Signaling Technology (Danvers, MA). LC3B (L7543) rabbit primary antibody was purchased from Sigma-Aldrich. PVDF membranes were incubated with 1:1000 dilutions of the primary antibodies overnight (4°C) in a shaking rotator. Membranes were washed three times with PBS and then incubated with a 1:5000 dilution of either goat anti-rabbit or goat anti-mouse horse radish peroxidase-conjugated secondary antibodies (Millipore, Billerica, MA) for 1 h at room temperature. Washing steps were repeated before adding clarity Western ECL substrate (Bio-Rad) for 5 min, after which the membranes were digitally photographed using a ChemiDoc MP Gel Doc system (Bio-Rad).

2.7. Senescence assay

LNCaP and C42B cells were cultured in their respective media in 6-well CellBind culture plates (Corning Inc.) at a density of 7.5 x 10^5 cells/well. After treatment with DIM or ring-DIMs,

senescent cells were detected using a Senescence β-galactosidase staining kit (Cell Signaling) according to the manufacturer's instructions. Cells were cultured in 6-well plates and treated with DIM or ring-DIMs for 24 h. Cells were washed with 1X PBS, then fixed with 1X Fixative Solution. Cells were then washed with 1X PBS and stained with β-galactosidase staining solution. Plates were incubated at 37°C overnight in a non-humidified incubator. Cells positive for β-galactosidase activity were counted by light microscopy under 100 X magnification in at least triplicate using different cell passages for each treatment. At least 50 cells per treatment were counted.

2.8. Electron microscope analysis

C42B cells were cultured in RPMI medium supplemented with 2% dextran-coated charcoal-stripped FBS and seeded in 6-well CellBind culture plates (Corning Inc.) at a density 7.5 x 10^5 cells/well. Cells were treated with DIM or ring-DIMs for 8 h and then fixed using 2.5% glutaraldehyde in 0.1 M phosphate buffer at pH 7.2 for 15 min. Cells were scraped with a rubber policeman, transferred to 1.5 ml tubes and centrifuged for 3 min at 1200 rpm. The cells were washed 3 times for 15 min with 3% sucrose in 0.1 M cacodylate buffer. Cells were fixed with freshly prepared 1.3 % (w/v) osmium tetroxide in collidine buffer for 1-2 hours. Fixed cells were dehydrated by successive passage through 25, 50, 75, 95 and 100 % solutions of acetone in water (15-30 minutes each), then embedded in SPURR resin mixtures (Mecalab, Montreal, QC). The block containing fixed cells were cut and encapsulated in mold filled with SPURR resin. Ultrathin sections were prepared with an ultramicrotome (LKB, Sollentuna, Sweden) and placed onto copper grids. After staining with uranyl acetate and lead citrate, sections were examined using a Hitachi H-7100 transmission electron microscope.

2.9. Statistical analyses

All experiments were performed at least 3 times independently using different cell passages. Treatments were performed in at least triplicate per experiment. Data are presented as mean ± SEM. Statistically significant differences ($p < 0.05$) between groups were determined using a one-way analysis of variance (ANOVA) followed by Dunnett's post-hoc test to correct for multiple comparisons to vehicle control. All data were analyzed using GraphPad Prism (version 5.01, GraphPad Software, San Diego, CA).

3. RESULTS

3.1. DIM and ring-DIMs induce the formation of autophagic vacuoles in prostate cancer cells

An 8-h treatment of androgen-sensitive LNCaP and androgen-insensitive C42B cells with DIM, 4,4'-Br_2DIM and 7,7'-Cl_2DIM significantly increased the formation of autophagic vacuoles (Figure 1A-D). The concentrations used in these experiments were based on our previous studies on DIM- and ring-DIM-mediated induction of protective autophagy in the same prostate cancer cells [8, 9]. We also confirmed the formation of autophagosomes by transmission electron microscopy after exposure of C42B cells to DIM and the ring-DIMs for 8 h (Figure 1E).

3.2. DIM and ring-DIMs induce autophagy via activation of AMPK signaling

To investigate the mechanism of DIM- and ring-DIM-mediated autophagy, we determined their effects on AMPK signaling. DIM and ring-DIMs significantly increased the conversion of LC3BI to LC3BII (LC3B-II/I ratio) in LNCaP and C42B cells (Figure 2A, B, S2B, S3B). In LNCaP cells, a time-dependent increase of AMPK phosphorylation by 4,4'-Br_2DIM was observed, whereas DIM significantly induced phosphorylation of AMPK only after treatment for 1 and 4 h, with levels decreasing after 8 h of exposure; however, 7,7'-Cl_2DIM treatment didn't change the levels of AMPK phosphorylation (Figure 2A, S2A). DIM and ring-DIMs significantly and time dependently increased AMPK phosphorylation in C42B cells at all time-points (Figure 2B, S3 A). Activation of AMPK signaling was confirmed in both cell lines by assessing the phosphorylation of its substrate acetyl-CoA carboxylase, ACC (Figure 2A, B, S2A, S3A). Next, we assessed whether the stimulation of AMPK activity resulted in an increased autophagic response by activating the autophagy initiator ULK1. We found that DIM and the ring-DIMs increased ULK1 phosphorylation time-dependently in both LNCaP and C42B cells (Figure 2A,

B, S2B, S3B). Pretreatment of cells with an ULK1 inhibitor (MRT67307, 10 μM) significantly sensitized LNCaP and C42B cells to cell death in the presence of sub-toxic concentrations of DIM or ring-DIMs (Figure 2C, D).

To confirm the role of AMPK signaling in the autophagy induced by DIM and the ring-DIMs, siRNA was used to inhibit *AMPK* gene expression. The increased conversion of LC3BI to LC3BII (LC3BII/I ratio) after a 24-h exposure of LNCaP to DIM or ring-DIMs and C42B cells to ring-DIMs was inhibited when cells were pretreated with *AMPK*-selective siRNA, while pretreatment of C42B cells exposed to DIM with AMPK siRNA didn't affect LC3BII/I ratio (Figure 3A, B, C, D). The siRNA-mediated inhibition of AMPK expression sensitized LNCaP and C42B cells to the cytotoxicity of normally sub-toxic concentrations of DIM and ring-DIMs (Figure 3E, F).

3.3. DIM and ring-DIMs promote autophagy via induction of AEG-1

Since AEG-1 is an upstream regulator of AMPK [20, 21], we therefore investigated the effect of DIM and ring-DIMs on induction of AEG-1 and AMPK-mediated autophagy. DIM induced AEG-1 expression in a time-dependent manner in both LNCaP and C42B cells (Figure 4A, B, C, D). 4,4'-Br_2DIM , and 7,7'-Cl_2DIM time dependently increased AEG-1 levels in LNCaP and C42B cells after a 1- and 4-h exposure, an effect that was no longer seen after 8 h. (Figure 4A, B, C, D). Pretreatment of LNCaP and C42B cells with *AEG-1*-selective siRNA inhibited DIM- and ring-DIM-mediated LC3BI-to-LC3BII conversion (Figure 5A, B, C, D) and sensitized LNCaP and C42B cells to the cytotoxicity of normally sub-toxic concentrations of DIM or ring-DIMs (Figure 5E, F). To know whether AEG-1 acts upstream or downstream of AMPK, ACC phosphorylation (a substrate uniquely phosphorylated by AMPK) was measured in LNCAP and

C42B cells exposed to DIM or ring-DIMs in the presence or absence of pretreatment with AEG-1 siRNA. Our results showed that inhibition of AEG-1 using selective siRNA reduced AMPK activation based on the phosphorylation of ACC (Fig 5A, B, C, D), which indicates that AEG-1 is an upstream regulator of AMPK.

3.4. Downregulation of AEG-1 induces senescence in LNCaP and C42B cells

To further explore the role of AEG-1 in DIM- and ring-DIM-mediated cytotoxicity, we assessed the effect of AEG-1 downregulation in LNCaP and C42B cells on their response to cytotoxic concentrations of DIM and ring-DIMs. Interestingly, siRNA-mediated silencing of AEG-1 expression protected LNCaP and C42B cells against the toxicity of DIM and ring-DIMs (Fig 6A, B). AEG-1 may affect multiple pathways related to cancer progression; hence, we investigated the effect of AEG-1 downregulation on cellular senescence. Pretreatment with AEG-1-selective siRNA promoted senescence as indicated by increased β-galactosidase activity in LNCaP (Fig 6C, E) and C42B (Fig 6D, F) cells treated with toxic concentrations of DIM and ring-DIMs. Induction of senescence was also confirmed by investing the effect of AEG-1 siRNA on cell proliferation of LNCaP and C42B cells treated with DIM. Our results showed a significant inhibition of cell proliferation in LNCaP and C42B cells pretreated with AEG-1 siRNA and then treated with DIM compared to DMSO control cells.

4. DISCUSSION

Our current findings demonstrate that DIM and ring-DIMs activate the AMPK signaling in LNCaP and C42B cells by increasing AMPK-, ACC-(a substrate uniquely phosphorylated by AMPK) and ULK1 phosphorylation in a time-dependent manner (Fig 2). Chen and coworkers previously reported that a formulated DIM (B-DIM), which has increased bioavailability *in vivo*,

can activate AMPK signaling as early as 3 h after exposure [25]. DIM has also been shown to activate AMPK signaling in ovarian cancer cells, and that this activation was required for induction of autophagy by DIM [26]. In our study, inhibition of AMPK expression using siRNA inhibited DIM- and ring-DIM-mediated conversion of LC3BI-to-LC3BII, indicating that the induction of autophagy by each of these compounds is dependent on AMPK activation (Fig 3). We found that the autophagy induced by DIM and ring-DIMs is cytoprotective in nature, since inhibition of either AMPK or ULK1 expression sensitized LNCaP and C42B cells, which underwent significant cell death in the presence of normally sub-toxic concentrations of DIM or ring-DIMs. The results confirm our earlier observations that pre-treatment of prostate cancer cells with the autophagy inhibitors bafilomycin A1 or 3-methyladenine also sensitized the cells to sub-toxic concentrations of DIM and ring-DIMs, suggesting a protective role of the autophagic response to DIM and ring-DIMs [9]. Our pervious study showed a concentration-dependent induction of autophagy after a 24-h exposure to DIM or ring-DIMs [9]. Results in Figure 1 show that formation of autophagic vacuoles in LNCaP and C42B cells are observed after an 8-h exposure to DIM and ring-DIMs. *In vivo* studies to assess co-treatment of natural compound like DIM with autophagy inhibitors in various (prostate) cancer models would determine the potential to increase anticancer efficacy of such combined therapies.

AEG-1 is overexpressed in various tumors including the prostate [20, 27] and contributes to chemoresistance in hepatocellular carcinoma (HCC) cells by increasing the expression of multi-drug resistance 1 (MDR1) gene [22], and knockdown of AEG-1 inhibits chemoresistance in cervical cancer cells [28]. Our present study reveals a novel mechanism of action for DIM- and ring-DIM-induced autophagy in human prostate cancer cells, which occurs via induction of AEG-1. We have shown that DIM and ring-DIMs increase AEG-1 protein levels time-dependently in

both LNCaP and C42B cells (Fig 4) and that the resultant induction of autophagy is dependent on AEG-1 (Fig 5). Inhibition of AEG-1 using siRNA repressed AMPK activation, indicating that AEG-1 is an upstream regulator of AMPK in prostate cancer cells. In line with our results, AEG-1 has been previously shown to induce protective autophagy via activation of AMPK in response to cellular metabolic stress in immortalized primary human fetal astrocytes (IM-PHFA) and in a human malignant glioma cell line (T98G) [20, 21]. In addition, AEG-1 overexpression was found to enhance autophagy in malignant glioma cells undergoing TGFβ1-induced endothelial-mesenchymal transition [27]. Kikuno and coworkers showed that downregulation of AEG-1 induced apoptosis in LNCaP and PC3 prostate cancer cells through upregulation of FOXO3a activity [29]. As another example, the natural product cryptotanshinone (derived from *Salvia miltiorrhiza*) was found to exert antitumor activity via inhibition of AEG-1 in hypoxic AI PC-3 prostate cancer cells [30]. Indeed, our current findings show that AEG-1 silencing sensitizes LNCaP and C42B cells to cell death mediated by sub-toxic concentrations of DIM and ring-DIMs. Thus, the induction of AEG-1 would appear to be a cell protection mechanism against the cellular stress and cytotoxicity caused in response to DIM and ring-DIMs in prostate cancer cells.

DIM targets multiple pathways associated with cancer progression *in vitro* and *in vivo* [31-33], and our findings provide further insight into the complexity of the mechanisms of anticancer action of DIM, as well as more potent synthetic DIM derivatives in prostate cancer cells. Charcoal-stripped serum (CSS) was used instead of fetal bovine serum (FBS) to minimize the level of androgens and other hormones to which the cells would be exposed [34]. The CSS culture medium of LNCaP cells was supplemented with 0.1 nM DHT to stimulate their androgen-dependent growth in a defined manner. The AD LNCaP and AI C42B prostate cancer cells had similar patterns of autophagy induction, activation of AMPK and AEG-1 induction, upon

treatment with DIM and ring-DIMs indicating a negligible effect of androgen signaling on the observed mechanisms. Interestingly we observed a protective effect after siRNA-mediated downregulation of AEG-1 against overtly cytotoxic concentrations of DIM or ring-DIMs in both LNCaP and C42B cells, which is contrast to our observed sensitization at subtoxic concentrations. Moreover, this protective effect of AEG-1 silencing was accompanied by induction of senescence in LNCaP and C42B cells treated with toxic concentration of DIM or ring-DIMs (Fig 6). Previous studies have shown that overexpression of AEG-1 inhibits senescence in hepatocytes isolated from transgenic mice by inhibiting the DNA damage response [23]. Senescent cells undergo irreversible proliferative arrest, which may inhibit tumor progression [30, 35, 36]. Accumulating evidence suggests that therapies directed at inducing senescence may improve cancer treatment outcomes [36-39]. Our study reveals that DIM- and ring-DIM-mediated induction of senescence and/or apoptosis is dependent on AEG-1, and induction of AEG-1 may be a key molecular switch that regulates the fate of prostate cancer cells either to undergo apoptosis or senescence (Fig 7). More studies are needed to assess the mechanism(s) of inhibition of senescence by AEG-1 and to determine the potential benefits of agents that induce senescence in treatment prostate cancer.

5. CONCLUSION

We have identified a novel mechanism of DIM- and ring-DIM-induced protective autophagy, which is clue to induction of AEG-1 and subsequent activation of AMPK. Our results suggest that development of novel drug therapies against prostate cancer could include selective autophagy inhibitors as adjuvants. Moreover, targeting DIM- and ring-DIM-mediated induction of AEG-1 and subsequent induction of senescence may be an effective novel therapy for treating prostate cancer.

ACKNOWLEDGMENTS

This work was funded by an operating grant from the Canadian Institutes of Health Research (CIHR grant no. MOP-115019) to JTS, EG and SS.. HD received a fellowship from the *Fonds de Recherche du Québec - Santé* (FRQS). All authors declare to have no conflicts of interest.

References

[1] J. Ferlay, I. Soerjomataram, R. Dikshit, S. Eser, C. Mathers, M. Rebelo, D.M. Parkin, D. Forman, F. Bray, Cancer incidence and mortality worldwide: sources, methods and major patterns in GLOBOCAN 2012, International journal of cancer 136(5) (2015) E359-86.
[2] R.L. Siegel, K.D. Miller, A. Jemal, Cancer statistics, 2016, CA: a cancer journal for clinicians 66(1) (2016) 7-30.
[3] D.K. Wysowski, J.P. Freiman, J.B. Tourtelot, M.L. Horton, 3rd, Fatal and nonfatal hepatotoxicity associated with flutamide, Annals of internal medicine 118(11) (1993) 860-4.
[4] D.G. McLeod, Tolerability of Nonsteroidal Antiandrogens in the Treatment of Advanced Prostate Cancer, The oncologist 2(1) (1997) 18-27.
[5] D.G. McLeod, E.D. Crawford, E.P. DeAntoni, Combined androgen blockade: the gold standard for metastatic prostate cancer, European urology 32 Suppl 3 (1997) 70-7.
[6] L.F. Bjeldanes, J.Y. Kim, K.R. Grose, J.C. Bartholomew, C.A. Bradfield, Aromatic hydrocarbon responsiveness-receptor agonists generated from indole-3-carbinol in vitro and in vivo: comparisons with 2,3,7,8-tetrachlorodibenzo-p-dioxin, Proc Natl Acad Sci U S A 88(21) (1991) 9543-7.
[7] K. Abdelbaqi, N. Lack, E.T. Guns, L. Kotha, S. Safe, J.T. Sanderson, Antiandrogenic and growth inhibitory effects of ring-substituted analogs of 3,3'-diindolylmethane (ring-DIMs) in hormone-responsive LNCaP human prostate cancer cells, Prostate 71(13) (2011) 1401-12.
[8] A.A. Goldberg, V.I. Titorenko, A. Beach, K. Abdelbaqi, S. Safe, J.T. Sanderson, Ring-substituted analogs of 3,3'-diindolylmethane (DIM) induce apoptosis and necrosis in androgen-dependent and -independent prostate cancer cells, Invest New Drugs 32(1) (2014) 25-36.
[9] A.A. Goldberg, H. Draz, D. Montes-Grajales, J. Olivero-Verbel, S.H. Safe, J.T. Sanderson, 3,3'-Diindolylmethane (DIM) and its ring-substituted halogenated analogs (ring-DIMs) induce differential mechanisms of survival and death in androgen-dependent and -independent prostate cancer cells, Genes Cancer 6(5-6) (2015) 265-80.
[10] C.W. Wang, D.J. Klionsky, The molecular mechanism of autophagy, Mol Med 9(3-4) (2003) 65-76.
[11] D. Glick, S. Barth, K.F. Macleod, Autophagy: cellular and molecular mechanisms, J Pathol 221(1) (2010) 3-12.
[12] E. White, The role for autophagy in cancer, J Clin Invest 125(1) (2015) 42-6.
[13] S.Y. Yang, M.C. Winslet, Dual role of autophagy in colon cancer cell survival, Ann Surg Oncol 18 Suppl 3 (2011) S239.
[14] C.B. Blackadar, Historical review of the causes of cancer, World journal of clinical oncology 7(1) (2016) 54-86.
[15] N. Mizushima, T. Yoshimori, Y. Ohsumi, The role of Atg proteins in autophagosome formation, Annu Rev Cell Dev Biol 27 (2011) 107-32.
[16] T.E. Hansen, T. Johansen, Following autophagy step by step, BMC Biol 9 (2011) 39.
[17] J. Kim, M. Kundu, B. Viollet, K.L. Guan, AMPK and mTOR regulate autophagy through direct phosphorylation of Ulk1, Nat Cell Biol 13(2) (2011) 132-41.

[18] G. Hu, Y. Wei, Y. Kang, The multifaceted role of MTDH/AEG-1 in cancer progression, Clinical cancer research : an official journal of the American Association for Cancer Research 15(18) (2009) 5615-20.
[19] X. Shi, X. Wang, The role of MTDH/AEG-1 in the progression of cancer, International journal of clinical and experimental medicine 8(4) (2015) 4795-807.
[20] S.K. Bhutia, T.P. Kegelman, S.K. Das, B. Azab, Z.Z. Su, S.G. Lee, D. Sarkar, P.B. Fisher, Astrocyte elevated gene-1 induces protective autophagy, Proc Natl Acad Sci U S A 107(51) (2010) 22243-8.
[21] S.K. Bhutia, T.P. Kegelman, S.K. Das, B. Azab, Z.Z. Su, S.G. Lee, D. Sarkar, P.B. Fisher, Astrocyte elevated gene-1 activates AMPK in response to cellular metabolic stress and promotes protective autophagy, Autophagy 7(5) (2011) 547-8.
[22] B.K. Yoo, D. Chen, Z.Z. Su, R. Gredler, J. Yoo, K. Shah, P.B. Fisher, D. Sarkar, Molecular mechanism of chemoresistance by astrocyte elevated gene-1, Cancer Res 70(8) (2010) 3249-58.
[23] J. Srivastava, A. Siddiq, L. Emdad, P.K. Santhekadur, D. Chen, R. Gredler, X.N. Shen, C.L. Robertson, C.I. Dumur, P.B. Hylemon, N.D. Mukhopadhyay, D. Bhere, K. Shah, R. Ahmad, S. Giashuddin, J. Stafflinger, M.A. Subler, J.J. Windle, P.B. Fisher, D. Sarkar, Astrocyte elevated gene-1 promotes hepatocarcinogenesis: novel insights from a mouse model, Hepatology 56(5) (2012) 1782-91.
[24] Y. Gong, H. Sohn, L. Xue, G.L. Firestone, L.F. Bjeldanes, 3,3'-Diindolylmethane is a novel mitochondrial H(+)-ATP synthase inhibitor that can induce p21(Cip1/Waf1) expression by induction of oxidative stress in human breast cancer cells, Cancer Res 66(9) (2006) 4880-7.
[25] D. Chen, S. Banerjee, Q.C. Cui, D. Kong, F.H. Sarkar, Q.P. Dou, Activation of AMP-activated protein kinase by 3,3'-Diindolylmethane (DIM) is associated with human prostate cancer cell death in vitro and in vivo, PLoS One 7(10) (2012) e47186.
[26] P.K. Kandala, S.K. Srivastava, Regulation of macroautophagy in ovarian cancer cells in vitro and in vivo by controlling glucose regulatory protein 78 and AMPK, Oncotarget 3(4) (2012) 435-49.
[27] M. Zou, W. Zhu, L. Wang, L. Shi, R. Gao, Y. Ou, X. Chen, Z. Wang, A. Jiang, K. Liu, M. Xiao, P. Ni, D. Wu, W. He, G. Sun, P. Li, S. Zhai, X. Wang, G. Hu, AEG-1/MTDH-activated autophagy enhances human malignant glioma susceptibility to TGF-beta1-triggered epithelial-mesenchymal transition, Oncotarget 7(11) (2016) 13122-38.
[28] X. Liu, D. Wang, H. Liu, Y. Feng, T. Zhu, L. Zhang, B. Zhu, Y. Zhang, Knockdown of astrocyte elevated gene-1 (AEG-1) in cervical cancer cells decreases their invasiveness, epithelial to mesenchymal transition, and chemoresistance, Cell Cycle 13(11) (2014) 1702-7.
[29] N. Kikuno, H. Shiina, S. Urakami, K. Kawamoto, H. Hirata, Y. Tanaka, R.F. Place, D. Pookot, S. Majid, M. Igawa, R. Dahiya, Knockdown of astrocyte-elevated gene-1 inhibits prostate cancer progression through upregulation of FOXO3a activity, Oncogene 26(55) (2007) 7647-55.
[30] H.J. Lee, D.B. Jung, E.J. Sohn, H.H. Kim, M.N. Park, J.H. Lew, S.G. Lee, B. Kim, S.H. Kim, Inhibition of Hypoxia Inducible Factor Alpha and Astrocyte-Elevated Gene-1 Mediates Cryptotanshinone Exerted Antitumor Activity in Hypoxic PC-3 Cells, Evidence-based complementary and alternative medicine : eCAM 2012 (2012) 390957.
[31] X. Ge, S. Yannai, G. Rennert, N. Gruener, F.A. Fares, 3,3'-Diindolylmethane induces apoptosis in human cancer cells, Biochemical and biophysical research communications 228(1) (1996) 153-8.
[32] M. Nachshon-Kedmi, F.A. Fares, S. Yannai, Therapeutic activity of 3,3'-diindolylmethane on prostate cancer in an in vivo model, Prostate 61(2) (2004) 153-60.
[33] M. Nachshon-Kedmi, S. Yannai, F.A. Fares, Induction of apoptosis in human prostate cancer cell line, PC3, by 3,3'-diindolylmethane through the mitochondrial pathway, British journal of cancer 91(7) (2004) 1358-63.
[34] J.P. Sedelaar, J.T. Isaacs, Tissue culture media supplemented with 10% fetal calf serum contains a castrate level of testosterone, Prostate 69(16) (2009) 1724-9.
[35] G.P. Dimri, What has senescence got to do with cancer?, Cancer cell 7(6) (2005) 505-12.

[36] M. Lee, J.S. Lee, Exploiting tumor cell senescence in anticancer therapy, BMB reports 47(2) (2014) 51-9.
[37] J.A. Ewald, J.A. Desotelle, G. Wilding, D.F. Jarrard, Therapy-induced senescence in cancer, Journal of the National Cancer Institute 102(20) (2010) 1536-46.
[38] A. Gibadulinova, M. Pastorek, P. Filipcik, P. Radvak, L. Csaderova, B. Vojtesek, S. Pastorekova, Cancer-associated S100P protein binds and inactivates p53, permits therapy-induced senescence and supports chemoresistance, Oncotarget 7(16) (2016) 22508-22.
[39] J. Tato-Costa, S. Casimiro, T. Pacheco, R. Pires, A. Fernandes, I. Alho, P. Pereira, P. Costa, H.B. Castelo, J. Ferreira, L. Costa, Therapy-Induced Cellular Senescence Induces Epithelial-to-Mesenchymal Transition and Increases Invasiveness in Rectal Cancer, Clinical colorectal cancer 15(2) (2016) 170-178 e3.

Figure legends

Figure 1: **DIM, 4,4'-Br_2DIM and 7,7'-Cl_2DIM induce autophagic vacuole formation in LNCaP (A) and C42B (B) cells after an 8-h exposure.** Autophagic vacuoles were detected using a Cyto-ID autophagy detection kit and nuclei were counterstained with Hoechst 33342 as described in Materials and Methods. LNCaP cells were treated with 20 µM DIM, 15µM 4,4'-Br_2DIM or 15 µM 7,7'-Cl_2DIM, whereas C42B cells were treated with 30 µM DIM, 15µM 4,4'-Br_2DIM or 20µM 7,7'-Cl_2DIM. Red arrows indicate representative examples of autophagic vacuoles stained with Cyto-ID. Scale bar = 50 µm. Fluorescence images are representative of three independent experiments. Number of autophagic vacuoles counted per cell in LNCaP (**C**) and C42B (**D**) cells are presented as means ± SEM of three independent experiments, each performed in triplicate. Statistically significant difference (**P*<0.05, ***P*<0.01) were determined by one-way ANOVA and a Dunnett posthoc test to correct for multiple comparisons to control. Transmission electron microscopic images of C42B cells treated with DIM, 4,4'-Br_2DIM or 7,7'-Cl_2DIM (E) for 8 h. Red arrows indicate autophagic vacuoles. Scale bar = 500 nm. ER = endoplasmic reticulum, M = mitochondria, PM = plasma membrane, N = nucleus.

Figure 2: **DIM and ring-DIMs induce phosphorylation of AMPK, ACC, ULK1 and the conversion of LC3BI to II in LNCaP (A) and C42B (B) cells.** LNCaP cells were exposed for 0, 1, 4, 8 h to 30 µM DIM, 20µM 4,4'-Br_2DIM or 20 µM 7,7'-Cl_2DIM whereas C42B cells were 0065posed to concentration s of 50 µM DIM, 20 µM 4,4'-Br_2DIM or 30 µM 7,7'-Cl_2DIM. Each gel is representative of three independent experiments. Percentage of intact LNCaP (C) and C42B (D) cells treated with DIM or ring-DIMs for 24 h with or without a 4-h pretreatment with ULK-1 inhibitor MRT 67307. Percentages are presented as means ± SEM of three independent experiments. Statistically significant difference (**P*<0.05, ***P*<0.01, ****P*<0.001) were

determined by one-way ANOVA and a Dunnett posthoc test to correct for multiple comparisons to control.

Figure 3: **DIM and ring-DIMs mediated autophagy is dependent on AMPK.** Levels of AMPK and LC3BI/II in LNCaP (A, C) and C42B (B, D) cells exposed to DIM, or ring-DIMs for 24 h with or without a 24-h pretreatment with AMPK siRNA. LNCaP and C42B cells were treated with 20 μM DIM, 15 μM 4,4'-Br_2DIM or 15 μM 7,7'-Cl_2DIM. Each gel is representative of three independent experiments. Percentage of intact LNCaP (E) and C42B (F) cells treated with DIM or ring-DIMs for 24 h with or without a 24-h pretreatment with AMPK siRNA. Results are representative of three independent experiments and shown as mean ± SEM. Statistically significant difference (**P*<0.05, ***P*<0.01) were determined by one-way ANOVA and a Dunnett posthoc test to correct for multiple comparisons to control.

Figure 4: **DIM and ring-DIMs induce AEG-1 in LNCaP and C42B cells.** AEG-1 and LC3BI/II levels in LNCaP (A, C) and C42B (B, D) cells treated for 24 h with DIM, 4,4'-Br_2DIM or 7,7'-Cl_2DIM. LNCaP cells were treated with 30 μM DIM, 20μM 4,4'-Br_2DIM or 20μM 7,7'-Cl_2DIM, whereas C42B cells were treated with 50 μM DIM, 20μM 4,4'-Br_2DIM or 30μM 7,7'-Cl_2DIM. Statistically significant difference (**P*<0.05, ***P*<0.01) were determined by one-way ANOVA and a Dunnett posthoc test to correct for multiple comparisons to control.

Figure 5: **DIM- and ring-DIM-mediated autophagy is dependent on AEG-1.** Levels of AEG-1, phospho-ACC, and LC3BI/II in LNCaP (A, C) and C42B (B, D) cells exposed to DIM, 4,4'-Br_2DIM or 7,7'-Cl_2DIM for 24 h with or without a 24-h pretreatment with AEG-1 siRNA.

LNCaP and C42B cells were treated with 20 µM DIM, 15 µM 4,4'-Br_2DIM or 15 µM 7,7'-Cl_2DIM. Each gel is representative of three independent experiments. Percentage of intact LNCaP (E) and C42B (F) cells after a 24-h exposure to DIM, 4,4'-Br_2DIM or 7,7'-Cl_2DIM with or without a 24-h pretreatment with AEG-1 siRNA. Percentages are presented as means ± SEM of three independent experiments. Statistically significant difference (*P<0.05, **P<0.01) were determined by one-way ANOVA and a Dunnett posthoc test to correct for multiple comparisons to control.

Figure 6: Percentage of intact LNCaP (A) and C42B (B) cells exposed to DIM, 4,4'-Br_2DIM or 7,7'-Cl_2DIM for 24 h with or without a 24-h pretreatment with AEG-1 siRNA. Senescence in LNCaP (C) and C42B (D) cells after a 24 h exposure to DIM, 4,4'-Br_2DIM and 7,7'-Cl_2DIM with or without a 24 h pretreatment with AEG-1 siRNA. LNCaP cells were treated with 20 µM DIM, 15 µM 4,4'-Br_2DIM or 15 µM 7,7'-Cl_2DIM, whereas C42B cells were treated with 30 µM DIM, 15 µM 4,4'-Br_2DIM or 20 µM 7,7'-Cl_2DIM. Senescence was measured using a senescence β-galactosidase staining kit as described in materials and methods. Images are representative of three independent experiments. Scale bar = 50 µm. Percentage of β-galactosidase-positive LNCaP (E) and C42B (F) cells treated as described above. Percentages are presented as means ± SEM of three independent experiments. Statistically significant difference (*P<0.05, ** P<0.01, ***P<0.001) were determined by one-way ANOVA and a Dunnett posthoc test to correct for multiple comparisons to control.

.

Figure 7: A schematic representation of the proposed mechanism of DIM-, 4,4'-Br_2DIM- and 7,7'-Cl_2DIM- mediated induction of protective autophagy in human prostate cancer cells.

Figure S1: Cell proliferation of LNCaP (A) and C42B (B) cells exposed to DIM with or without a 24-h pretreatment with AEG-1 siRNA.

Figure S2: Protein levels of pAMPK, pACC, ULK1, LC3BI and LC3BII (expressed as LC3BII/I ratio) in LNCaP cells after a 0, 1, 4, 8 h of exposure to DIM, 4,4'-Br_2DIM or 7,7'-Cl_2DIM. Quantification of protein bands densitometry was carried out using ImageJ 1.6 software (Wayne Rasband, NIH)

Figure S3: Protein levels of pAMPK, pACC, ULK1 LC3BI and LC3BII (expressed as LC3BII/I ratio) in C42B cells after 0, 1, 4, 8 h of exposure to DIM, 4,4'-Br_2DIM or 7,7'-Cl_2DIM. Quantification of protein bands densitometry was carried out using ImageJ 1.6 software (Wayne Rasband, NIH)

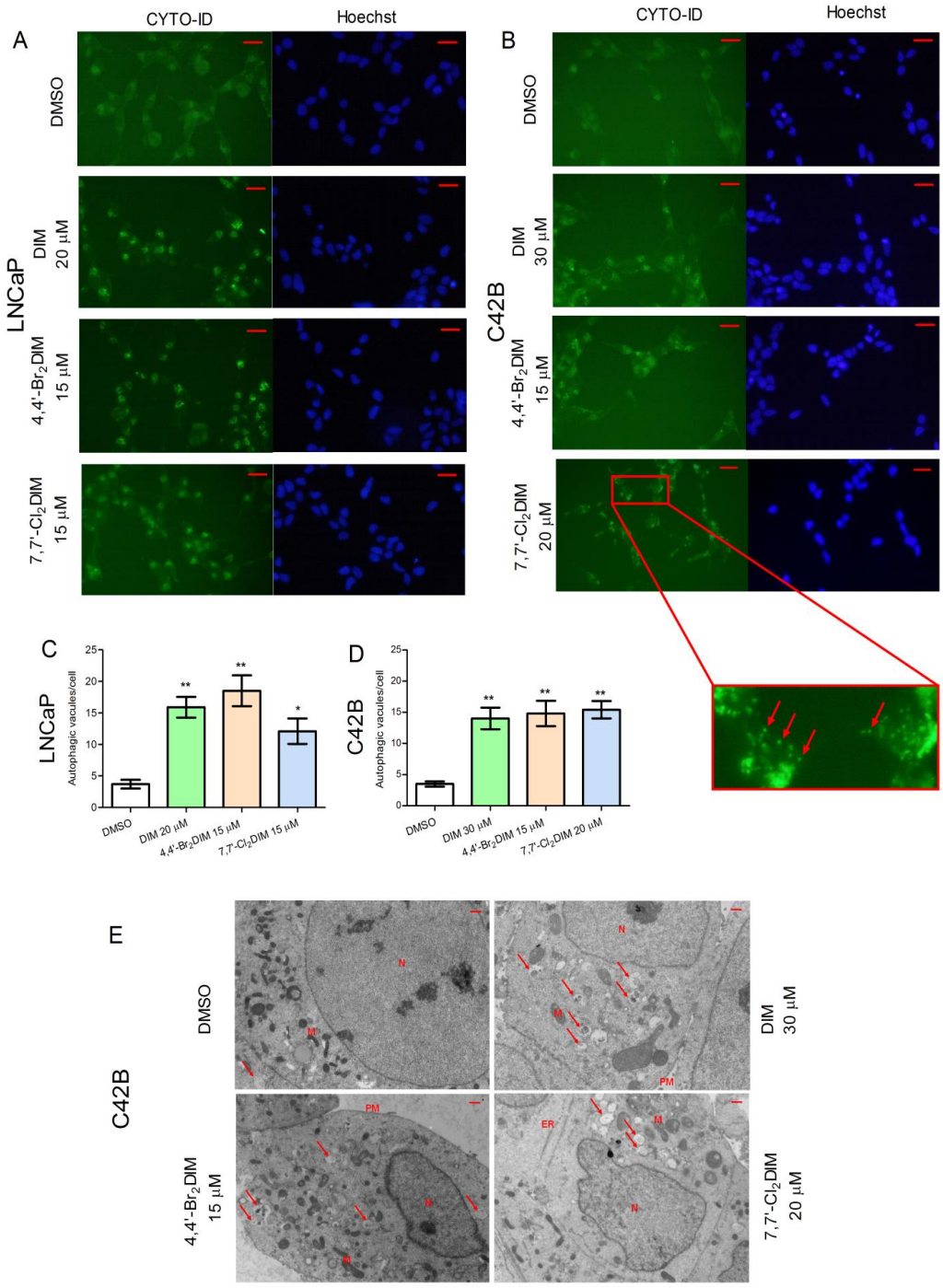

Fig. 1

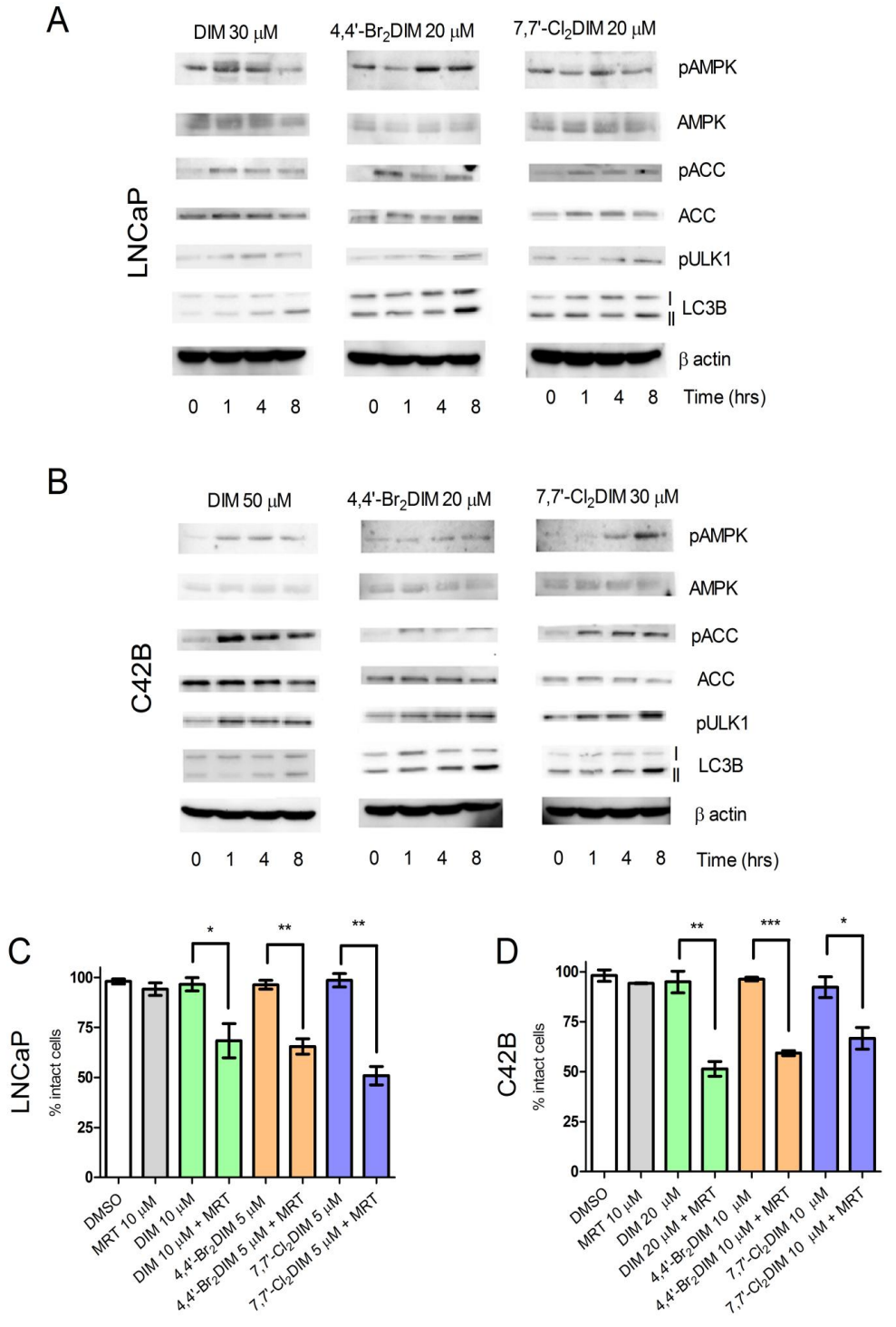

Fig. 2

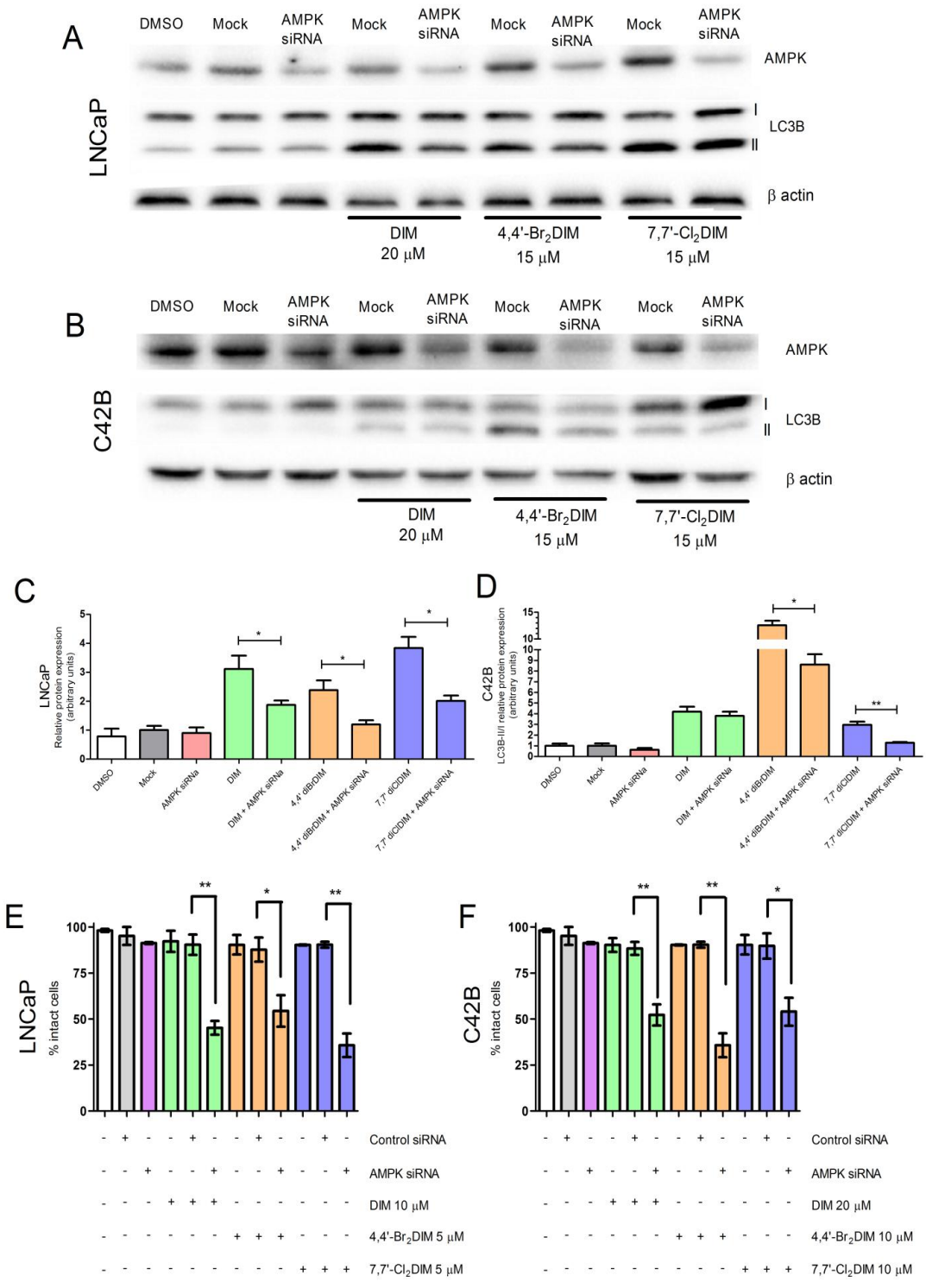
A
DMSO
Mock
AMPK siRNA
Mock
AMPK siRNA
Mock
AMPK siRNA
Mock
AMPK siRNA
LNCaP
AMPK
LC3B
I
II
β actin
DIM 20 μM
4,4'-Br2DIM 15 μM
7,7'-Cl2DIM 15 μM
B
C42B
C
LNCaP
Relative protein expression (arbitrary units)
D
C42B
LC3B-II/I relative protein expression (arbitrary units)
DMSO
Mock
AMPK siRNa
DIM
DIM + AMPK siRNa
4,4' diBrDIM
4,4' diBrDIM + AMPK siRNA
7,7' diClDIM
7,7' diClDIM + AMPK siRNA
E
LNCaP
% intact cells
F
C42B
Control siRNA
AMPK siRNA
DIM 10 μM
DIM 20 μM
4,4'-Br2DIM 5 μM
4,4'-Br2DIM 10 μM
7,7'-Cl2DIM 5 μM
7,7'-Cl2DIM 10 μM

Fig. 3

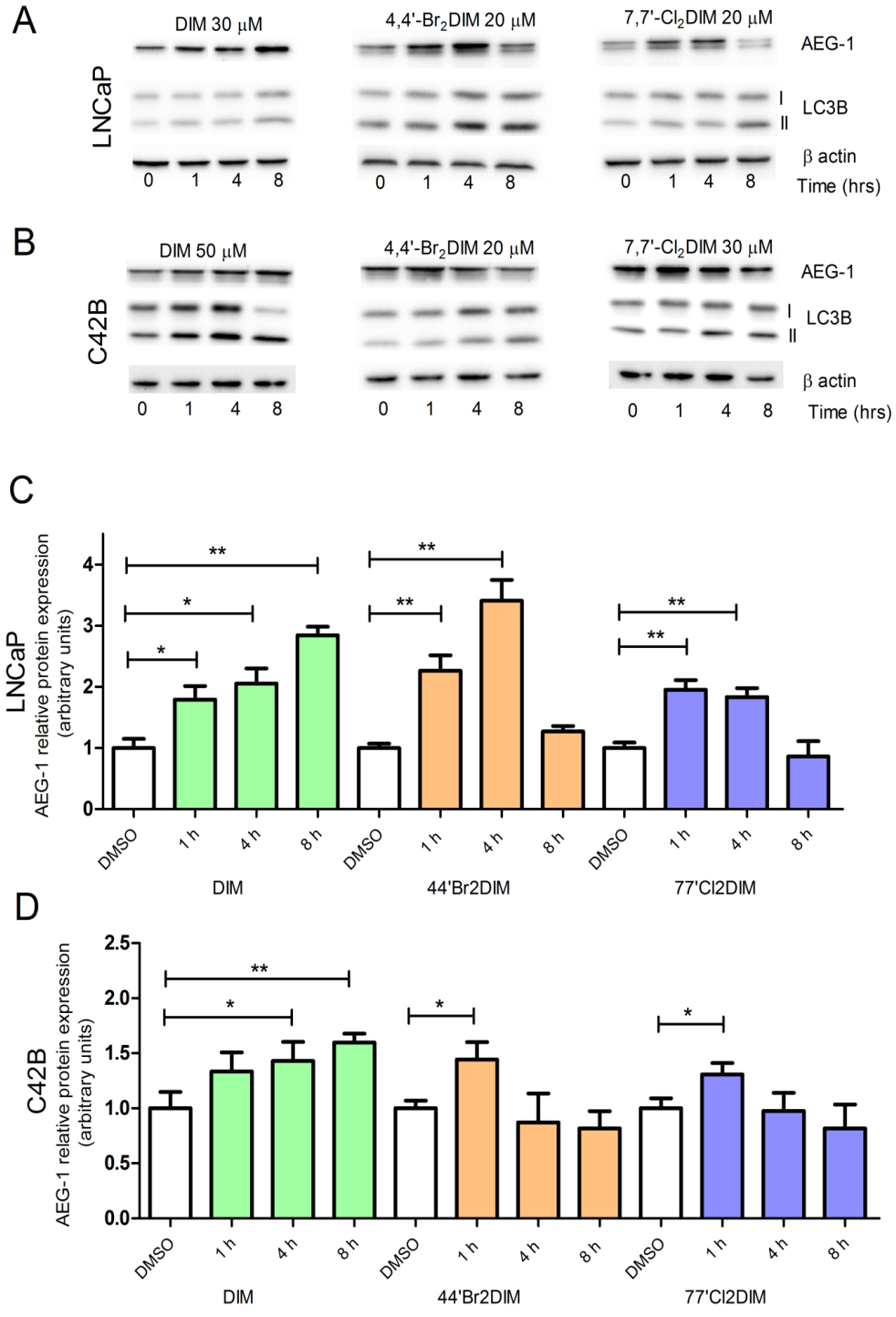

Fig. 4

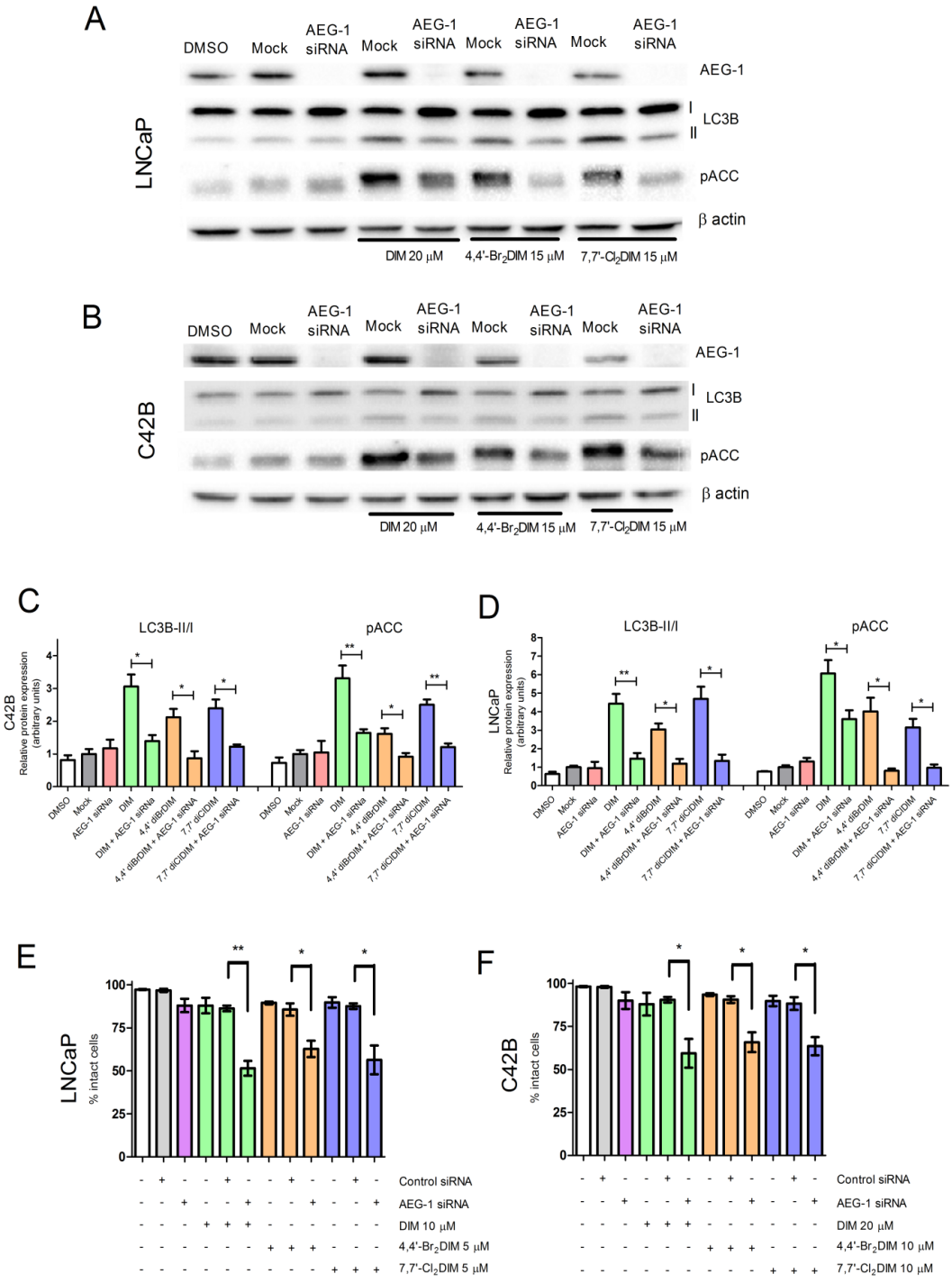

Fig. 5

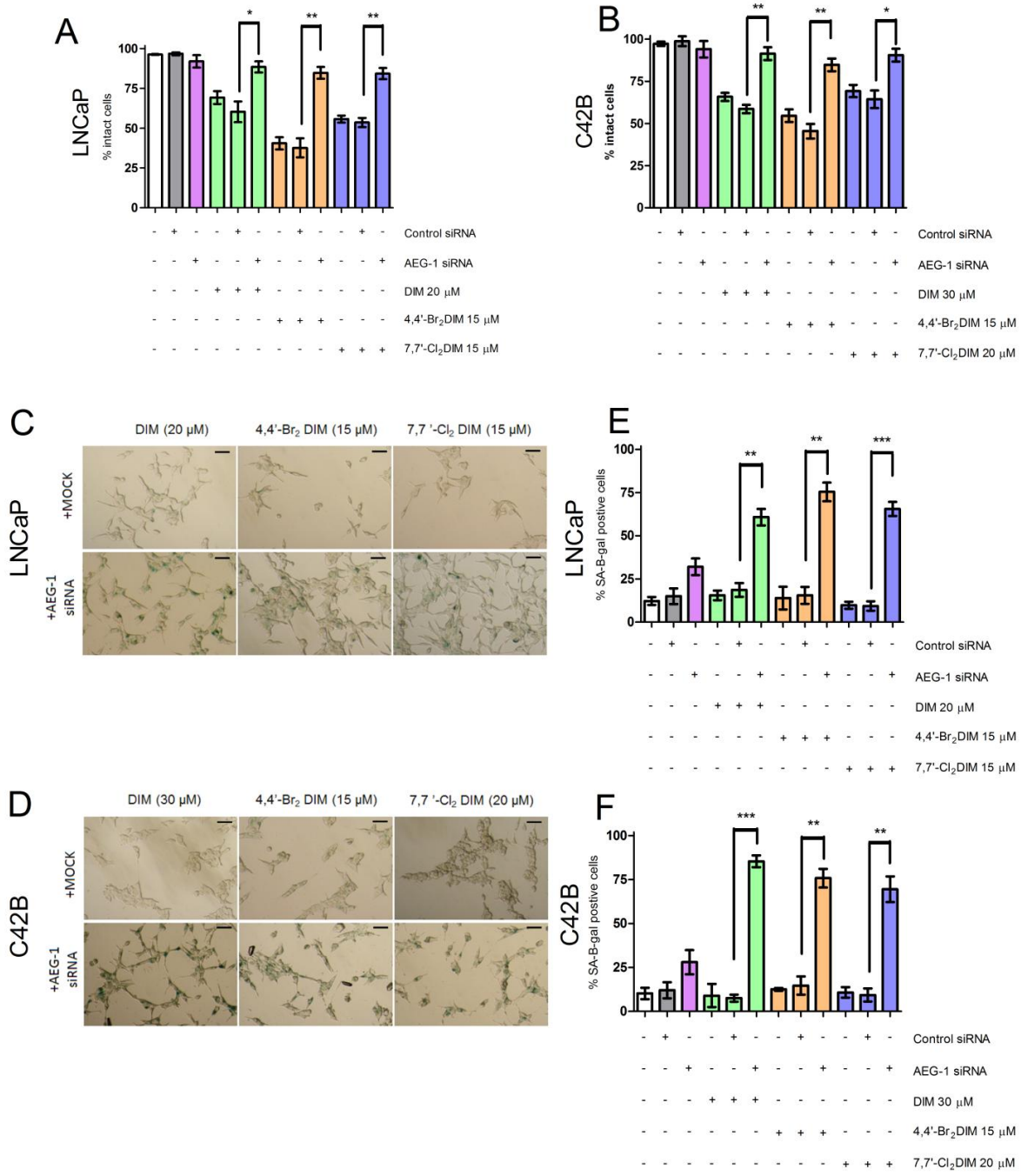

Fig. 6

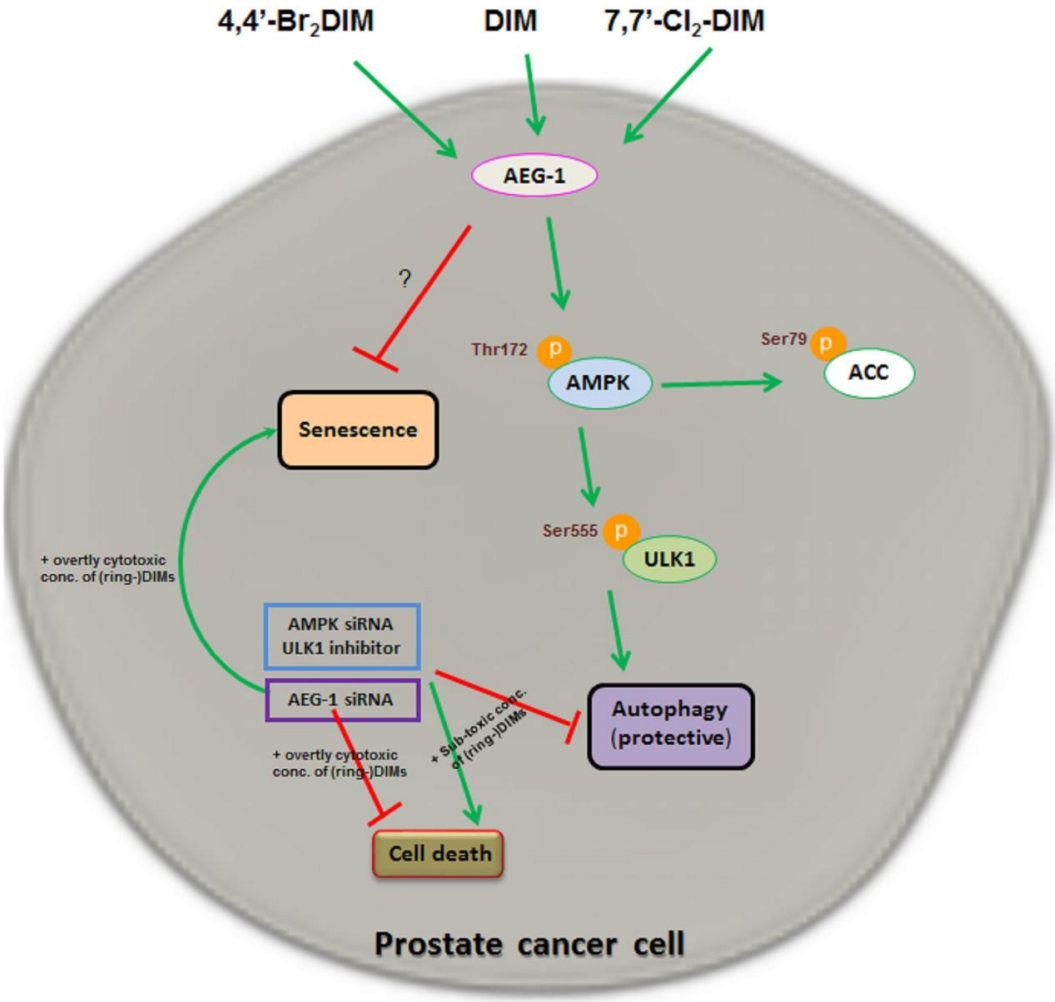

Fig. 7

Highlights

(1) DIM and ring-DIMs induce the formation of autophagic vacuoles in prostate cancer cells.

(2) Inhibition of either AEG-1 or AMPK expression sensitizes prostate cancer cells, which underwent significant cell death in the presence of normally sub-toxic concentrations of DIM or ring-DIMs.

(3) DIM- and ring-DIM-induced protective autophagy is mediated through the induction of the oncogenic protein AEG-1 and subsequent activation of AMPK.

(4) Downregulation of AEG-1 induces senescence in prostate cancer cells.